Effect of Si^{4+} substitution on structure and luminescence of Eu^{2+}-doped $Na_2CaMg(PO_4)_2$ phosphors

YONGYAN XU[a,c*], KAI ZHANG[b,**], YING CHANG[a], CHUN CHANG[c]
[a]*College of Chemistry and Chemical Engineering, Zhoukou Normal University, Zhoukou 466001, China*
[b]*College of Physics, Zhoukou Normal University, Zhoukou 466001, China*
[c]*College of Chemical Engineering and Energy, Zhengzhou University, Zhengzhou 450001, China*

The Eu^{2+}-doped $Na_2CaMg(P_{1-x}Si_xO_4)_2$ phosphors were prepared by high-temperature solid-state reaction. The structural and optical effects of Si^{4+} substitution were investigated with the use of X-ray diffraction, Fourier transform infrared spectra, Raman spectra, luminescence spectra and fluorescence decay curves, etc. The spectral parameters, Stokes shift and Eu^{2+} substitution sites in $Na_2CaMg(PO_4)_2$ were discussed by using empirical equations. The results show that Si^{4+} substitution increases the emission intensity of Eu^{2+} by ca. 50% at the optimal concentration of x = 0.05. This study can provide a guidance for the development of Eu^{2+}-activated phosphate phosphors for WLEDs.

(Received March 7, 2020; accepted November 25, 2020)

Keywords: Si^{4+} substitution, Luminescence, Eu^{2+}-doped $Na_2CaMg(PO_4)_2$, WLEDs

In recent studies, it has been found that colloidal semiconductor quantum dots, such as cadmium sulfide, indium phosphide and perovskite quantum dots, have a broad application prospect in the development of white light-emitting diodes (WLEDs) due to their advantages of adjustable emission color, low cost and environmental friendliness [1-2]. However, the rare earth or manganese ions activated inorganic compounds are still concentrated researcher's attention as efficient phosphors, because of their high chemical and physical stability, excellent thermal stability, rigid crystal structure and other advantages [3-4].

Divalent europium (Eu^{2+}) ion, with the characteristics of wide emission band, small stokes displacement, short attenuation time, and large influence by matrix, is used as the main activator of commercial phosphors at present [5-7]. By adjusting the lattice environment around the luminescence centers, the emission color of Eu^{2+} -activated phosphors can be tuned between ultraviolet and red. The emission color and intensity of phosphors are important indicators to determine their application. At present, there are many reports about the emission color tuning of Eu^{2+}, but there are few reports about optimizing the emission intensity without changing the emission color [8-9].

Presently, in several studies it was shown that the Eu^{2+}-doped $M_3MgSi_2O_8$ (M= Ca/ Sr/Ba) orthosilicate with a glaserite-type monoclinic structure can emit strong blue light, and this material is considered as a candidate product for high-performance phosphors [10]. However, the orthosilicate phosphors often need for a high preparation temperature. In comparison to that, phosphate compounds require a lower preparation temperature. Therefore, phosphors based on phosphate matrix have attracted much attention in recent years. Interestingly, phosphate $Na_2CaMg(PO_4)_2$ also has a glaserite-type monoclinic layered structure. Researchers have explored the luminescence properties of $Na_2CaMg(PO_4)_2$ doped with rare earth ions and found that the Eu^{2+}-doped $Na_2CaMg(PO_4)_2$ phosphors have good thermal stability and broad application potential in ultraviolet-based WLED [12-14]. The emission color of Eu^{2+}-doped $Na_2CaMg(PO_4)_2$ phosphors can be adjusted by co-doping other rare earth ions, manganese ions, or alkaline earth metal ions (Sr^{2+}, Ba^{2+}) [8,12,13]. However, the task to reach high enough emission intensity of Eu^{2+} is still a challenge. Phosphate and silicate are appropriate hosts for luminescent materials due to their structural diversity, higher thermal stability, and visible light transparency; therefore, it is proposed that the combination of these matrices would have similar advantages [15]. Inspired by the above works, we hope to synthesize a highly ordered glaserite-type phosphor based on the combination of phosphate and silicate to achieve high-quality lighting.

As far as we know, there is little earlier report on the effect of Si^{4+} substitution on structure and luminescence of Eu^{2+}-doped $Na_2CaMg(PO_4)_2$ phosphors. Thus, in the present study, the Eu^{2+}-doped $Na_2CaMg(P_{1-x}Si_xO_4)_2$ phosphors have been synthesized. The structure and spectral parameters of the Eu^{2+}-doped $Na_2CaMg(P_{1-x}Si_xO_4)_2$ phosphors will be discussed in detail. Respectively, this work can provide a guidance for the development of Eu^{2+}-activated phosphate phosphors for WLEDs.

Samples $Na_2CaMg(P_{1-x}Si_xO_4)_2$: $0.02Eu^{2+}$ (x=0-0.15) were synthesized by high-temperature solid-state reaction method. The starting reagents of Eu_2O_3 (99.99%), $(MgCO_3)_4{\cdot}Mg(OH)_2{\cdot}5H_2O$ (A.R.), Na_2CO_3 (A.R.), $CaCO_3$ (A.R.), $NH_4H_2PO_4$ (A.R.) and SiO_2 (A.R.) were supplied

by Shanghai Yien Chemical Technology Co., Ltd (Shanghai, China). The starting reagents were mixed according to stoichiometric ratios and ground together. First, the mixtures were preheated at 550 ℃ for 2 h in a muffle furnace. Then, the precursors were reground and sintered at 950 ℃ for 6 h under carbon monoxide reduction atmosphere. Upon cooling down to room temperature naturally, the final products were ground again for further measurements.

The XRD patterns were collected on a Bruker D8 Focus Advance X-ray diffractometer (Bruker, Germany) using Cu K_α radiation (λ=0.15406 nm). The Fourier transform infrared (FT-IR) spectra were measured by a FTIR 920 spectrometer (Tianjin Tuopu Instrument Co., Ltd.). Raman spectra were performed via an iRaman BWS415-532S spectrometer (BWTek, USA) with a 532 nm laser as the incident light. The excitation and emission spectra were measured via a LS55 fluorescence spectrophotometer (PerkinElmer, USA) equipped with a 150 W Xenon lamp. The fluorescence decay times were measured via a FLSP-920 spectrometer (Edinburgh Instruments, UK) at room temperature.

Earlier, it was reported that $Na_2CaMg(PO_4)_2$ with a glaserite-type monoclinic structure has two nine-coordinated (CN=9) Na^+ sites and one ten-coordinated (CN=10) Ca^{2+} site. The Na1-O distances, ranging from 2.258 to 2.896 Å, are slightly lower than the Na2-O distance in the range of 2.241-3.077Å. The Ca-O distances is in the range of 2.397-3.375Å. The radii of Ca^{2+} (1.23 Å for CN = 10) and Na^+ (1.24 Å for CN = 9) are similar to that of Eu^{2+} (1.3 Å for CN= 9, 1.35 Å for CN= 10) [12]. Therefore, either Na^+ or Ca^{2+} sites are likely to be replaced by Eu^{2+} ions. In theory, the percentage difference in radius (D_r) between doped and substituted ions can be used to evaluate the feasibility of substitution. Meanwhile, the D_r must be less than 30% to be replaced [16]. The D_r values between doped ions Eu^{2+} and substituted cations Na^+ or Ca^{2+} can be calculated using equation [17]:

$$Dr = \left| \frac{R_m(CN) - R_d(CN)}{R_m(CN)} \right| \times 100\% \quad (1)$$

where R_m(CN) and R_d (CN) represent the radius of the substituted cation and doped ions, respectively. The calculated D_r values are 4.84 % for Na^+ and 9.76 % for Ca^{2+}, which are all less than 30%. Therefore, both Ca^{2+} and Na^+ sites can be replaced by Eu^{2+} ions.

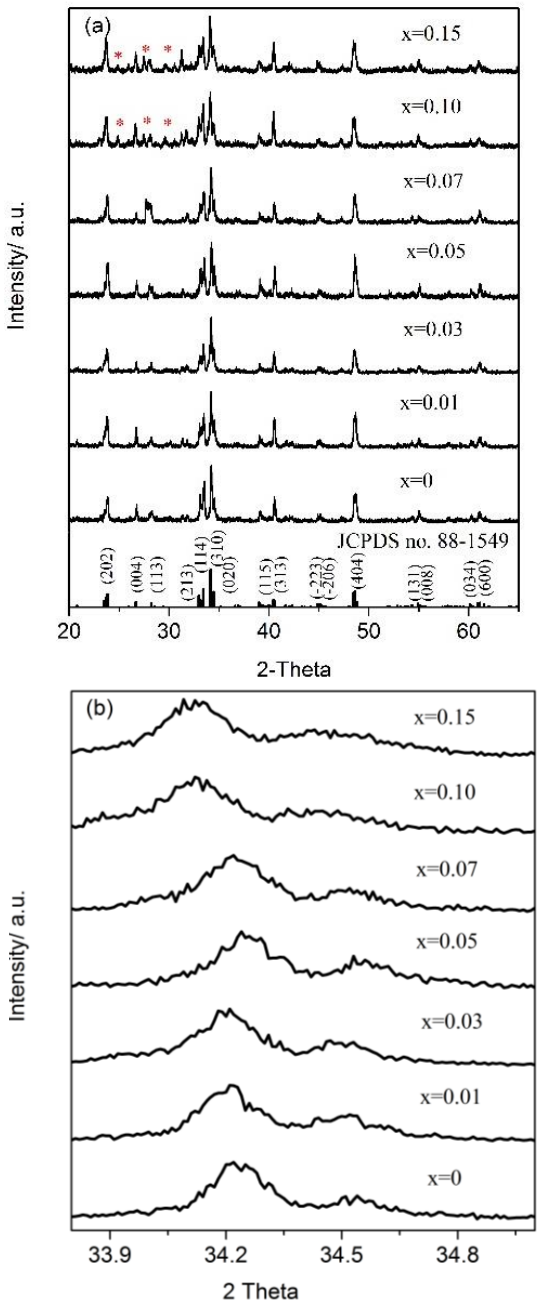

Fig. 1. (a) XRD patterns of $Na_2CaMg(P_{1-x}Si_xO_4)_2$: 0.02$Eu^{2+}$ (x=0-0.15) and JCPDS no. 88-1549 in the full range. (b) XRD patterns enlarged in the range of 33.8-35 degrees

The XRD patterns of $Na_2CaMg(P_{1-x}Si_xO_4)_2$: 0.02$Eu^{2+}$ (x=0-0.15) samples are shown in Fig. 1. The XRD patterns of $Na_2CaMg(P_{1-x}Si_xO_4)_2$: 0.02$Eu^{2+}$ (x=0-0.15) samples can be well matched with the standard card of $Na_2CaMg(PO_4)_2$ (JCPDS no. 88-1549) [12]. When doping level is greater than 0.07, the impure phase peaks appear as shown asterisks. Moreover, the main diffraction peaks shift to lower angles because the larger Si^{4+}(0.40 Å) ions replace P^{5+}(0.31 Å) ions into $Na_2CaMg(PO_4)_2$ lattice [18].

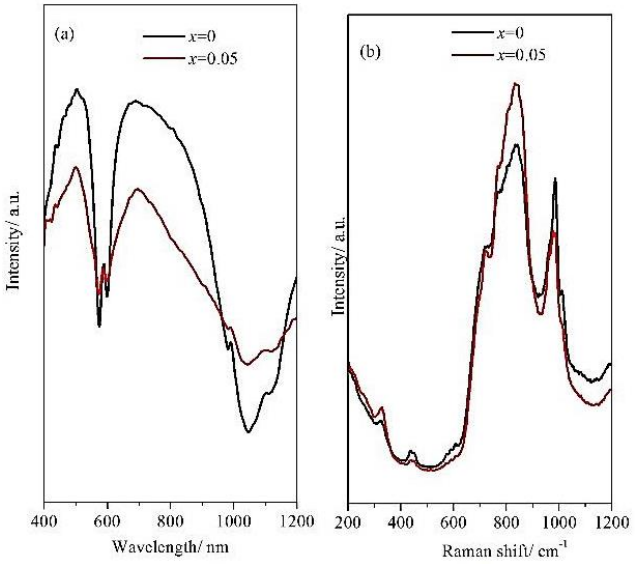

Fig. 2. The FT-IR and Raman spectra for $Na_2CaMg(P_{1-x}Si_xO_4)_2$: $0.02Eu^{2+}$ (x=0, 0.05)

To verify the existence of $(SiO_4)^{4-}$ in the products, the FT-IR and Raman spectra are measured. The FT-IR spectra of representative $Na_2CaMg(PO_4)_2$: $0.02Eu^{2+}$ and $Na_2CaMg(P_{0.95}Si_{0.05}O_4)_2$: $0.02Eu^{2+}$ samples are shown in Fig. 2(a). It can be seen that intense absorption bands appear at about 1120-940 cm^{-1} and 650-540 cm^{-1} in all samples. In general, the IR absorption bands of $[PO_4]$ is mainly located at 1120-940 cm^{-1} and 670-450 cm^{-1}, and those of $[SiO_4]$ at 1175-860 cm^{-1} and 570-410 cm^{-1} [19-20]. In Fig. 2(a), it can be seen that Si^{4+} substitution only makes the $[PO_4]$-derived absorption peaks broader. This is because that a small amount of Si^{4+} substitution produces the characteristic absorption bands of the $[SiO_4]$ tetrahedra, which are coupled with the absorption bands of $[PO_4]$, thus broadening the absorption range of the phosphate matrix. It is clear that $Na_2CaMg(PO_4)_2$: $0.02Eu^{2+}$ and $Na_2CaMg(P_{0.95}Si_{0.05}O_4)_2$: $0.02Eu^{2+}$ samples also exhibit similar Raman vibration spectra (as shown in Fig. 2(b)). In Si^{4+} substitutions samples, the vibration peak intensity in the range of 200-360 cm^{-1} and 750-880 cm^{-1} is remarkably enhanced due to O-Si-O bending modes and Si-O stretching, respectively [21]. Therefore, the results of XRD, FT-IR and Raman spectra show that Si^{4+} substitution has little effect on the structure of $Na_2CaMg(PO_4)_2$ matrix.

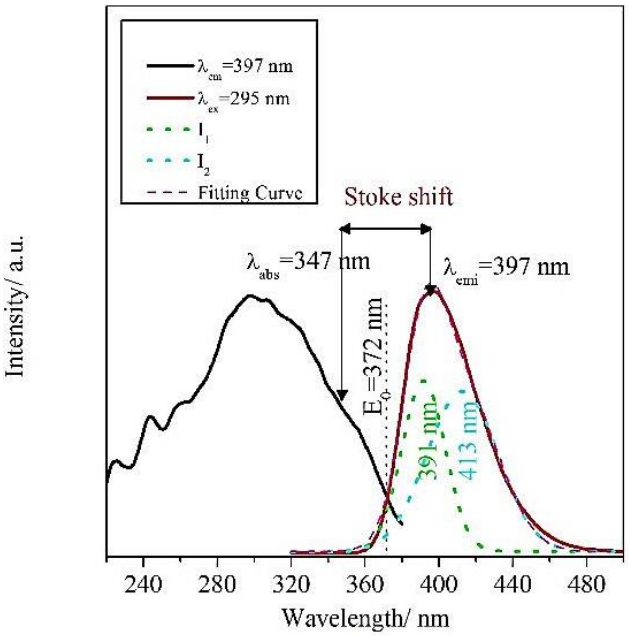

Fig. 3. The excitation (λ_{em} = 397 nm) and emission spectra (λ_{ex} = 295 nm) of $Na_2CaMg(PO_4)_2$: Eu^{2+}

As shown in Fig. 3, the excitation spectrum of $Na_2CaMg(PO_4)_2$: 0.02 Eu^{2+} sample monitored at 397 nm exhibits a strong broad band in the range of 220- 380 nm originating from $4f^7 \rightarrow 4f^65d^1$ transitions of Eu^{2+}. With varying the excitation wavelength, the emission spectra can be considered to stay invariable except the difference in emission intensity. For example, upon the excitation at 295 nm, the phosphor emits a broad emission band from 360 to 450 nm centering at about 397 nm, assigned to $4f^65d^1 \rightarrow 4f^7$ transition of Eu^{2+}. The asymmetric emission spectrum can be fitted by two Gaussian components, peaked at 391 and 413 nm, originating from two different Eu^{2+} emission centers. Since the emission wavelength of Eu^{2+} ions is closely related to the ligand field, each emission component corresponds to different crystallographic position. In order to determine the substitution sites assigned to each emission, the position in energy for the Eu^{2+} emission is calculated by the following empirical equations [22]:

$$E = Q[1-(\frac{V}{4})^{1/V}10^{-\phi}] \quad (2)$$

$$\phi = \frac{nrea}{80} \quad (3)$$

where n and V represent the coordination number and valence of Eu^{2+} ions, respectively; r is the host cation radius substituted by Eu^{2+} ion (in Å); Q is the position in energy for the lower d-band edge for the free Eu^{2+} ions (Q = 34,000 cm^{-1}); ea is the electron affinity of the atoms forming anions (in eV); E represents the position in energy

for the Eu^{2+} emission (cm^{-1}). Here ea is 2.5 eV [23], V is 2, the r of Ca^{2+} is 1.23 Å and Na^{+} is 1.24 Å. The fitting peaks and calculated values based on empirical equations (2) and (3) are listed in Table 1. Therefore, it can be considered that the emission peaks at 391 and 413 nm correspond to Ca^{2+} and Na^{+} sites, respectively [20]. Because the emission reflects the ligand field formed by the nearest oxide ions [24], in $Na_2CaMg(PO_4)_2$, the shortest bond length of Ca-O is 2.397 Å, and that of Na-O is 2.241 Å, which are all shorter than ideal values of 2.63 Å and 2.64 Å predicted by Shannon. Consequently, the fitting wavelength is smaller than that for the calculated value using empirical formulas.

Table 1. The calculated and Gaussian fitting peaks of Eu^{2+} ions in $Na_2CaMg(PO_4)_2$

	Coordination number	Radius (Å)	$E_{calculated}$ (cm^{-1})	$\lambda_{calculated}$ (nm)	Fitting peak (nm)
Ca^{2+}	10	1.23	24079	415	391
Na^{+}	9	1.24	23229	430	413

Dorenbos points out that the energy difference between the ground and excited states of the divalent lanthanide elements can be calculated using Eq. (4) and (5) [25].

$$E_{abs} = E_{free} - D \quad (4)$$

$$E_{emi} = E_{free} - D - \Delta S \quad (5)$$

where E_{free} is the energy for the free ion from the ground state to the excited state. D is the red-shift of the 5d orbital level, and ΔS is the Stokes shift. For $Na_2CaMg(PO_4)_2$: Eu^{2+}, E_{abs} is 3.57 eV (347 nm), E_{emi} is 3.12 eV (397 nm), E_{free} is 4.19 eV [16]. Thus, the red-shift $D = E_{free} - E_{emi}$ = 0.62 eV, the Stokes shift $\Delta S = E_{abs} - E_{emi} - D$ = 0.45 eV. There is an approximately linear relationship between the absorption and emission energies of Eu^{2+} and Ce^{3+} in the same matrix [25]. Therefore, the absorption and emission energy of Eu^{2+} can be approximated by the correlation value of Ce^{3+}.

$$E(Eu^{2+}) = (0.64 \pm 0.22) \times E(Ce^{3+}) + (0.53 \mp 0.06)\ eV \quad (6)$$

where $E(Ce^{3+})$ is 3.65 eV (340 nm) [26]. Therefore, according to Eq. (6), $E(Eu^{2+})$ is estimated to be 3.73 eV (332 nm). It can be seen that the difference between predicted and experimental results is not significant.

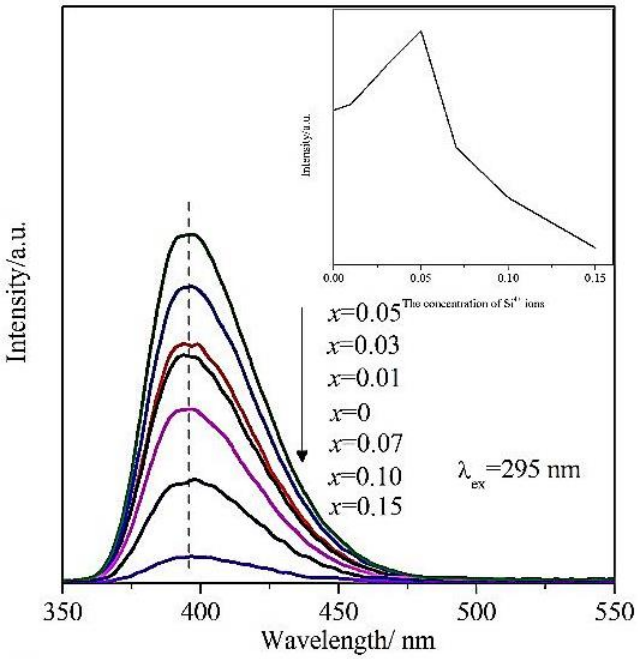

Fig. 4. The emission spectra (λ_{ex} = 295 nm) of $Na_2CaMg(P_{1-x}Si_xO_4)_2$: 0.02$Eu^{2+}$ (x=0- 0.15). The inset shows the dependence of the emission intensity on Si^{4+} doping concentration

Ion substitution is usually used to change the lattice environment around the luminescence center and thus improve the luminescence performance of phosphors [9]. A set of emission spectra of $Na_2CaMg(P_{1-x}Si_xO_4)_2$: 0.02 Eu^{2+} (x=0-0.15) samples with varying Si^{4+} content upon the excitation at 295 nm is displayed in Fig. 4. In $Na_2CaMg(PO_4)_2$: 0.02 Eu^{2+}, when a small amount of the P^{5+} is replaced by Si^{4+}, it is obvious that the emission intensity increases first and then decreases, but the position of the emission band is independent of different x value. This is because the substitution of P^{5+} ions with Si^{4+} ions produces more rigid structure, reducing the energy lost by phonon vibrations in the lattice, leading to an increase in the emission intensity [27]. There is no significant difference in ion radii of P^{5+} with Si^{4+} ions and, so the spectra do not show an obvious red shift. But impurity phase also appears with higher Si^{4+} content, which will result in the quenching of luminescence due to the reabsorption and energy transfer of impurity phase. The inset in Fig. 4 represents concentration dependence of the emission intensity of $Na_2CaMg(P_{1-x}Si_xO_4)_2$: 0.02 Eu^{2+}. Compared with $Na_2CaMg(PO_4)_2$: 0.02Eu^{2+}, the Si^{4+} substitution increases the emission intensity by ca. 50% at the optimized concentration of x = 0.05.

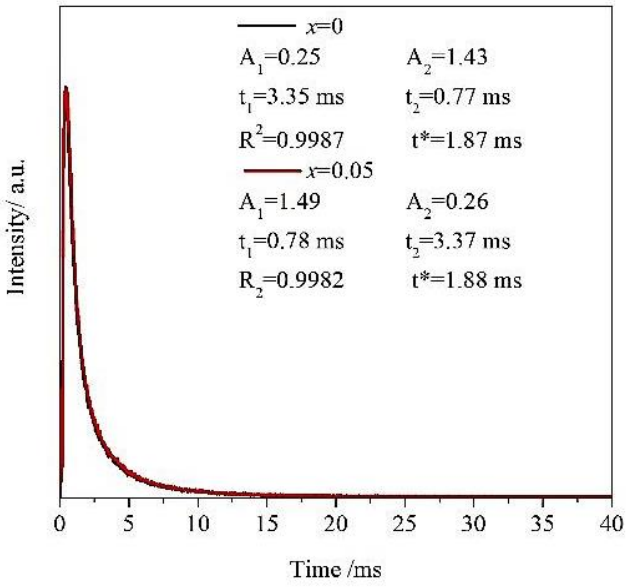

Fig. 5. The fluorescence decay curves (λ_{em} = 400 nm) of $Na_2CaMg(P_{1-x}Si_xO_4)_2$: 0.02$Eu^{2+}$ (x=0, 0.05) under the excitation of 295 nm

The fluorescence lifetimes of $Na_2CaMg(P_{1-x}Si_xO_4)_2$: 0.02 Eu^{2+} samples are measured. As shown in Fig. 5 (λ_{ex} = 295 nm, λ_{em} = 400 nm), the fluorescence decay curves can be well-fitted to a double exponential equation [28]:

$$I(t) = A_1 \exp(-t/\tau_1) + A_2 \exp(-t/\tau_2) \quad (7)$$

where I(t) is the fluorescence intensity at time t; A_1 and A_2 are constants; τ_1 and τ_2 are the lifetimes for the exponential components. Furthermore, the average lifetime (τ*) can be calculated by using the following equation [29]:

$$\langle \tau^* \rangle = (A_1\tau_1^2 + A_2\tau_2^2)/(A_1\tau_1 + A_2\tau_2) \quad (8)$$

Based on Eq. (8), the fluorescence decay times of $Na_2CaMg(PO_4)_2$: 0.02Eu^{2+} and $Na_2CaMg(P_{0.95}Si_{0.05}O_4)_2$: 0.02$Eu^{2+}$ samples are determined to be ca. 1.87 and 1.88 ms, respectively, indicating that Si^{4+} substitution reduces the non-radiative energy transfer.

In summary, a series of Eu^{2+} doped $Na_2CaMg(P_{1-x}Si_xO_4)_2$ phosphors was successfully synthesized and their structure and luminescent properties were investigated. The results show that there are two kinds of Eu^{2+} emission center occupied in $Na_2CaMg(PO_4)_2$ matrix, the emission peak at 391 nm corresponds to Ca site and that at 413 nm to Na site; the Stokes shift is 0.45 eV; the Si^{4+} substitution has no obvious effect on the structure, which increases the emission intensity by ca. 50% at *x*=0.05. The work can provide a new strategy for modulating luminescence performance of phosphate phosphor.

Acknowledgments

This study is supported by the High Level Personnel Fund of Zhoukou Normal University (ZKNUC2017042), Education Department of Henan Province Natural Science Research Program (182102311088) and the Scientific Innovation Fund Project of Zhoukou Normal University (ZKNUD2019075). The luminescence spectra and fluorescence decay curves from Henan Key Laboratory of Rare Earth Functional Materials were greatly appreciated.

References

[1] F. L. Yuan, Z. B. Wang, X. H. Li, Y. C. Li, Z. A. Tan, L. Z. Fan, S. H. Yang, Adv. Mater. **29**, 1604436 (2017).
[2] Y. Wei, Z. Y. Cheng, J. Lin, Chem. Soc. Rev. **48**, 310 (2019).
[3] R. J. Li, X. D. Xu, L. B. Su, Q. L. Sai, C. T. Xia, Q. H. Yang, J. Xu, A. Strzep, A. Pókoszek, Chin. Opt. Lett. **14**, 021602 (2016).
[4] Z. G. Xia, Y. Y. Zhang, M. S. Molokeev, V. V. Atuchin, J. Phys. Chem. C **117**, 20847 (2013).
[5] G. G. Li, C. C. Lin, W. T. Chen, M. S. Molokeev, V. V. Atuchin, C. Y. Chiang, W. Z. Zhou, C. W. Wang, W. H. Li, H. S. Sheu, T. S. Chan, C. G. Ma, R. S. Liu, Chem. Mater. **26**, 2991 (2014).
[6] J. Cheng, J. Zhang, J. Lu, X. T. Bian, H. C. Zhang, Z. H. Shen, X. W. Ni, P. C. Ma, J. Shi, Chin. Opt. Lett. **17**, 051602 (2019).
[7] J. W. Qiao, L. X. Ning, M. S. Molokeev, Y. C. Chuang, Q. Y. Zhang, K. R. Poeppelmeier, Z. G. Xia, Angew. Chem. **131**, 2 (2019).
[8] H. L. Zhang, D. W. Yuan, X. Y. Mi, X. Y. Zhang, Z. H. Bai, X. L. Liu, J. Lin, J. Alloy. Compd. **798**, 119 (2019).
[9] B. Q. Shao, J. S. Huo, H. P. You, Adv. Opt. Mater. **7**, 1900319 (2019).
[10] H. F. Yan, Z. X. Qiu, J. L. Zhang, L. P. Yu, S. X. Lian, Z. Y. Ma, W. L. Zhou, Ceram. Int. **45**, 16963 (2019).
[11] H. P. Ji, Z. H. Huang, Z. G. Xia, M. S. Molokeev, V. V. Atuchin, M. H. Fang, S. F. Huang, Inorg. Chem. **53** 5129 (2014).
[12] J. Zhou, Z. G. Xia, J. Lumin. **146**, 22 (2014).
[13] J. Lü, Y. L. Huang, Y. Tao, H. J. Seoc, Appl. Phys. A **99**, 859 (2010).
[14] Y. Yonesaki, C. Matsuda, J. Solid State Chem. **184**, 3247 (2011).
[15] X. G. Zhang, Z. Y. Guo, RSC Adv. **6**, 104311 (2016).
[16] S. Y. Wang, Q. Sun, B. Devakumar, L. L. Sun, J. Liang, X. Y. Huang, RSC Adv. **8**, 30191 (2018).
[17] Z. G. Xia, J. Zhou, Z. Y. Mao, J. Mater. Chem. C, **1**, 5917 (2013).
[18] J. Zou, B. B. Yang, S. M. Zhu, J. R. Li, F. C. Wang, J. Mater. Sci-Mater. El. **27**, 13199 (2016).
[19] Y. Wei, J. S. Gao, G. C. Xing, G. G. Li, P. P. Dang, S. S. Liang, Y. S. Huang, C. C. Lin, T. S. Chan, J.

Lin, Inorg. Chem. **58**, 6376 (2019).
[20] Y. Yonesaki, Q. Dong, N. S. B. Mohamad, A. Miura, T. Takei, J. J. Yamanaka, N. Kumada, N. Kinomura, J. Alloy. Compd. **509**, 8738 (2011).
[21] X. Y. Ji, J. L. Zhang, Y. Li, S. Z. Liao, X. G. Zhang, Z. Y. Yang, Z. L. Wang, Z. X. Qiu, W. L. Zhou, L. P. Yu, S. X. Lian, Chem. Mater. **30**, 5137 (2018).
[22] L. G. Van Uitert, J. Lumin. **29**, 1 (1984).
[23] Y. Yonesaki, T. Takei, N. Kumada, N. Kinomura, J. Lumin. **128**, 1507 (2008).
[24] G. Annadurai, S. Masilla Moses Kennedy, V. Sivakumar, Superlattice. Microst. **93**, 57 (2016).
[25] X. G. Zhang, F. W. Mo, L. Y. Zhou, M. L. Gong, J. Alloy. Compd. **575**, 314 (2013).
[26] J. Lü, Y. L. Huang, Y. Tao, H. J. Seoc, J. Alloy. Compd. **500**, 134 (2010).
[27] F. F. Zhang, K. X. Song, J. Jiang, S. Wu, P. Zheng, Q. M. Huang, J. M. Xu, H. B. Qin, J. Alloy. Compd. **615**, 588 (2014).
[28] K. Li, M. M. Shang, D. L. Geng, H. Z. Lian, Y. Zhang, J. Fan, J. Lin, Inorg. Chem. **53**, 6743 (2014).
[29] Y. Y. Xu, X. M. Li, W. L. Feng, W. L. Li, K. Zhang, Dalton T. **45**, 3983 (2016).

*Corresponding author: yongyanxu@163.com,
** zhangkaiswu@163.com